

2022

## **Carnot Analysis of Heat Pump Drying: Ideal Efficiency and Dry Time**

Kyle Gluesenkamp

*Oak Ridge National Laboratories, United States of America, [gluesenkampk@ornl.gov](mailto:gluesenkampk@ornl.gov)*

Viral Patel

Follow this and additional works at: <https://docs.lib.purdue.edu/iracc>

---

Gluesenkamp, Kyle and Patel, Viral, "Carnot Analysis of Heat Pump Drying: Ideal Efficiency and Dry Time" (2022). *International Refrigeration and Air Conditioning Conference*. Paper 2459.  
<https://docs.lib.purdue.edu/iracc/2459>

This document has been made available through Purdue e-Pubs, a service of the Purdue University Libraries. Please contact [epubs@purdue.edu](mailto:epubs@purdue.edu) for additional information. Complete proceedings may be acquired in print and on CD-ROM directly from the Ray W. Herrick Laboratories at <https://engineering.purdue.edu/Herrick/Events/orderlit.html>

## Carnot Analysis of Heat Pump Drying: Ideal Efficiency and Dry Time

Kyle R. GLUESENKAMP<sup>1\*</sup>, Viral K. PATEL<sup>1</sup>

<sup>1</sup>Oak Ridge National Laboratory, Buildings and Transportation Science Division,  
Oak Ridge, TN, USA  
[gluesenkampk@ornl.gov](mailto:gluesenkampk@ornl.gov)

\* Corresponding Author

### ABSTRACT

Drying processes are important in appliances and in industry, and clothes drying accounts for approximately 3% of residential primary energy consumption in the US. Globally, heat pump tumble dryers (HPD) are increasing their market share against the ubiquitous electric resistance tumble dryer (ERD). In this work, efficiency and dry time limits are defined for ideal HPDs, for both closed air cycle (unvented) and open air cycle (vented). These limits are compared with the limits for ERD. The traditional Carnot efficiency limit for an ideal heat pump, operating between a hot and a cold thermal reservoir, does not apply directly to clothes dryers. One reason dryers require a novel analysis is the presence of additional degrees of freedom, since the hot and cold temperatures are floating, unfixed by ambient conditions. Furthermore, dryers can operate in a closed or open air cycle, and each requires a different analysis. In the closed (unvented) case, the hot and cold temperatures are coupled to each other; while in the open (vented) case, the hot and cold temperatures are both independent free variables. This paper provides an analysis of the fundamental efficiency limits of ERDs and HPDs, which can inform the design and performance limits of evaporative drying technology.

### 1. INTRODUCTION

Clothes dryers function by heating air to remove moisture from fabric. The hot air interacts with the tumbling wet fabric in the dryer drum, where heat and mass transfer occur between the air and the fabric. Electric clothes dryer technologies have been developed over the years which utilize different methods of heating the air. The two most common electric dryers are electric resistance dryers (ERD) which use a simple heating element and heat pump tumble dryers (HPD), which use a compressor to circulate refrigerant through a vapor-compression cycle, and heat is transferred from the condenser to the dryer process air.

Detailed analyses of clothes drying processes have been conducted by many researchers in order to understand and optimize them. These studies include system-level thermodynamic analysis as well as component-level analysis involving closer study of the actual heat and mass transfer processes in different components of the dryers. From a system standpoint, for example, Peng et al. 2019 conducted a thermodynamic analysis of novel heat pump cycles for drying processes with large temperature lift. Beyond the single-stage heat pump cycle, they also considered a multi-temperature cascade cycle and combined single-stage cycle to address the problems associated with large temperature lifts, including insufficient heat output, high compression ratio, and low coefficient of performance (COP). They varied the operating parameters for the different cycles and optimized their performance, leading to increases in cycle

---

\* Corresponding author. Tel.: +1-865-241-2952.

*E-mail address:* [gluesenkampk@ornl.gov](mailto:gluesenkampk@ornl.gov)

Notice: This manuscript has been authored by UT-Battelle, LLC under Contract No. DE-AC05-00OR22725 with the U.S. Department of Energy. The United States Government retains and the publisher, by accepting the article for publication, acknowledges that the United States Government retains a non-exclusive, paid-up, irrevocable, world-wide license to publish or reproduce the published form of this manuscript, or allow others to do so, for United States Government purposes. The Department of Energy will provide public access to these results of federally sponsored research in accordance with the DOE Public Access Plan (<http://energy.gov/downloads/doe-public-access-plan>).

COPs of 95% and 88% for the multi-temperature cascade cycle and combined single-stage cycle compared to the single-stage compression cycle, respectively. They found that among the different thermodynamic cycles which were analyzed, the multi-temperature cascade cycle was the most promising to be used for drying equipment with large temperature lift and could potentially be retrofitted onto a conventional cycle.

Along these lines, modeling work has also been done on HPDs by other researchers for both the refrigerant-side and air-side: Lee et al. 2019 studied the effects of varying heat exchanger geometries and volumetric air flow rate on the suction/discharge pressures and COPs of a HPD; Sian and Wang. 2019 did a comparative study of HPDs by considering both conventional refrigerant (R134a) and CO<sub>2</sub> (R744) and they determined the resulting effects on specific moisture extraction rate (SMER), COP and drying time; Cao et al. 2021 developed a quasi-steady-state model of a closed-loop HPD consisting of a dynamic fabric drying model and a steady-state heat pump system model. They analyzed the effects of compressor size, area ratio of the evaporator to total, circulating air flow rate, condensing temperature upper bound, and refrigerant charge on the SMER and drying time and also performed optimization using the response surface method to improve these performance metrics.

From a component standpoint, Lee et al. 2022 have studied the heat and mass transfer characteristics in the drum of a tumble dryer both experimentally and using a prediction model. In experiments, they quantified heat and mass transfer of water from the clothes to the air, including the heat loss in the dryer drum, by measuring temperature, humidity, airflow rate, and water content of clothes. They showed that the mass transfer rate increased as the air temperature, airflow rate, and water content of clothes increased, but the enhancement was dominated by the temperature. By raising the temperature from 40°C to 80°C, the mass transfer rate increased from 196%–238%. The prediction models of heat and mass transfer of water and heat loss in the tumble drum were developed using an artificial neural network and showed optimal agreement with the measured data.

Despite the above studies in the general literature focusing on the actual heat and mass transfer processes in clothes dryers, the only thorough high-level theoretical treatment of a Carnot heat pump in the context of clothes drying found is in Gluesenkamp et al. 2020. Such an analysis is important because it helps to highlight the gap between actual dryer efficiency and what can be achieved as the Carnot limit is approached. The results of this analysis can be used along with other research to determine how much more the efficiency of both ERDs and HPDs can still be improved through optimization and changes in engineering design. Furthermore, the performance of clothes dryers is strongly affected by whether they are vented or unvented, and it is also an important practical matter which affects their design and installation cost. As such, it is essential to consider both vented and unvented performance in any detailed analysis of clothes dryers.

This work addresses the question, “what is the ideal efficiency for clothes drying?” Both non-heat pump and Carnot heat pump drying processes are considered. Compared with Gluesenkamp et al. 2020, in this work the degrees of freedom are analyzed in greater detail for each dryer type, and the results for each of the four types is presented in a more uniform way. In contrast to the very clean result for a simple Carnot heat pump, in which efficiency is simply  $T_H/(T_H - T_C)$ , the Carnot performance of clothes drying is surprisingly diverse. Since drying is an inherently transient process (the product must start wet and end dry), infinite efficiency is possible by using infinite dry time. Thus, any meaningful discussion of ideal drying performance must consider dry time. A variety of tradeoffs between efficiency and dry time are available for ideal drying cycles.

## 2. METHODOLOGY

In this section, four types of dryers are defined (section 2.1), performance metrics are introduced (section 2.2), and the assumptions shared by all four dryer types are described (sections 2.3 – 2.6).

### 2.1 Dryer types considered

In this work, four dryer types are discussed (two heat pump, and two non-heat pump). The four dryer types are shown schematically in **Figure 1**, with psychrometric state points indicated by numbers [1] through [5]. The state point nomenclature is defined such that state point [1] always indicates the surroundings, [2] indicates the condition entering the drum, and [3] indicates the condition leaving the drum. For each dryer type, additional state point numbers are added as needed, and there is no common meaning for state points [4] and [5].

Note that the process air stream for the two unvented dryers does not include ambient state point [1]. They interact with the ambient through an ambient HX. In contrast, the vented dryers start with process air at state point [1].

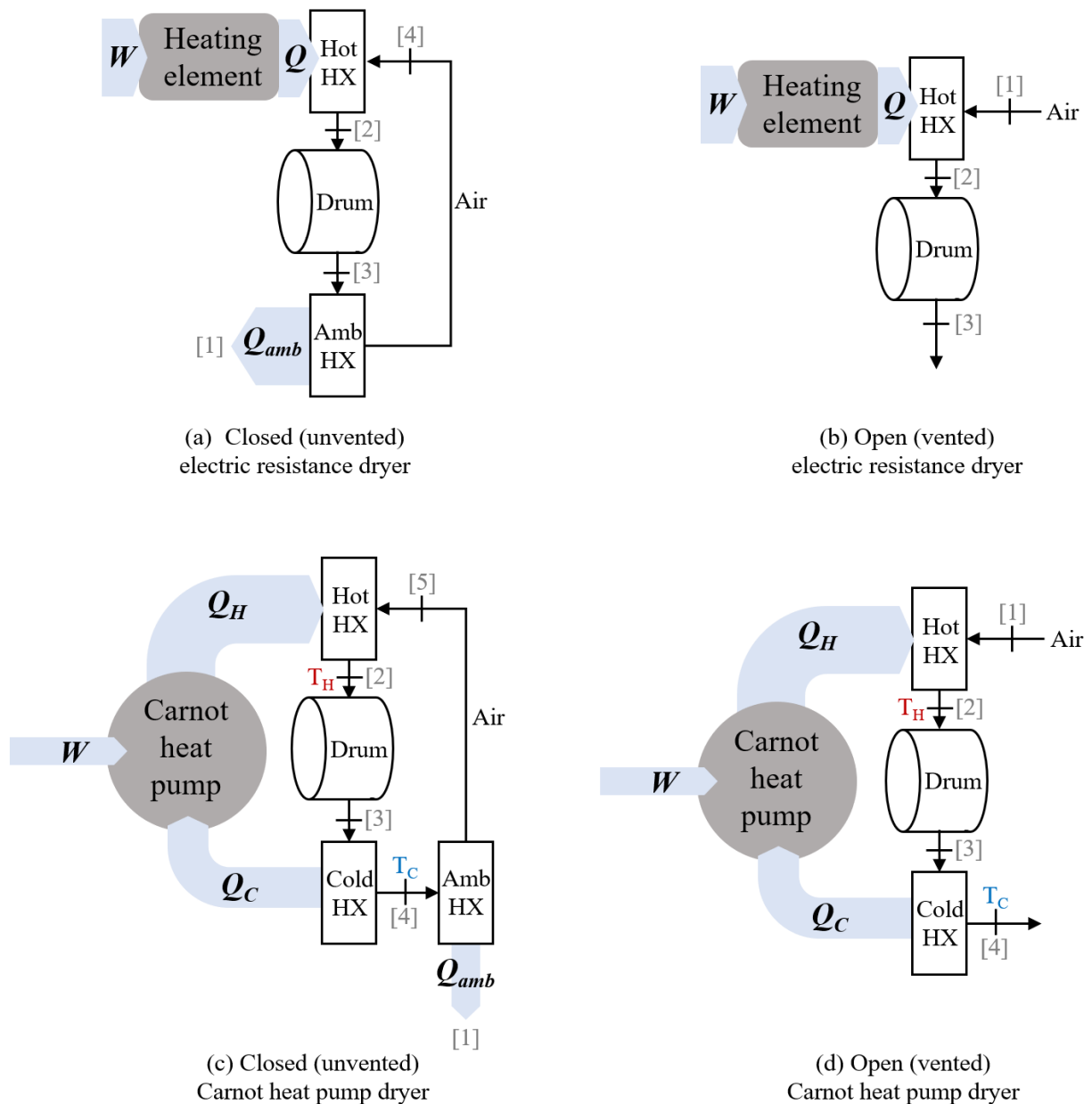


**Figure 1:** Four ideal dryer types: (a) unvented ERD, (b) vented ERD, (c) unvented Carnot HPD, and (d) vented Carnot HPD. Air flows are shown in black lines, energy flows are shown in blue arrows, and state points are indicated by numbers in square brackets.

## 2.2 Performance metrics

Drying efficiency is defined relative to a process in which each unit of work energy supplied to the dryer results in one unit of latent heat removed from the moisture in the cloth load (Eqn. 1).

$$\eta = \frac{m_{evap} h_{fg}}{W} \quad (1)$$

Drying time is non-dimensionalized as the g/s of water evaporated per g/s of air flow in the system. This can equivalently be expressed in terms of psychrometric humidity ratio, as in Eqn. 2.

$$\text{normalized drying rate} = \frac{\dot{m}_{evap}}{\dot{m}_{dry\ air}} = \frac{\dot{m}_{dry\ air}(\omega_3 - \omega_2)}{\dot{m}_{dry\ air}} = \Delta\omega \quad \left( \frac{g_w/s}{g_{da}/s} \text{ or } \frac{g_w}{g_{da}} \right) \quad (2)$$

### 2.3 Steady state process air

Real clothes drying is an inherently transient process, since the moisture content of the cloth is changing with time. In this work, the process air state points are considered to be in steady state.

In addition, all thermal masses are neglected in this work. Two categories of thermal mass are treated separately, as described in the following two paragraphs.

The thermal mass of the cloth is certainly an inherent aspect of the fundamental drying efficiency limit. However, cloth thermal mass impacts the evaporative efficiency by less than 3%, and is thus neglected to enhance to clarity of this work. The following calculation illustrates the small magnitude of impact of the thermal mass of the cloth itself. The specific heat capacity of cotton cloth is about 1.3 kJ/kg<sub>c</sub>-K. In an example where cloth is heating from 25 to 50°C, that requires a heat addition of 33 kJ/kg<sub>c</sub>. Let us compare that quantity of heat addition with the heat required to dry the same cloth from 57.5% to 4% moisture content: a reduction of 0.535 kg<sub>w</sub>/kg<sub>c</sub> multiplied by the latent heat of water (2450 kJ/kg<sub>w</sub>) means a heat addition of 1343 kJ/kg<sub>c</sub>. Thus, the total heat addition is 33 + 1343 = 1376 kJ/kg<sub>c</sub>. The sensible heat of raising the cloth temperature is only 2.4% of the total.

Regarding the thermal mass of the dryer appliance (drum, ducts, etc.), these are neglected since they contribute about 10% of the total energy to evaporatively dry cloth. An analysis was reported in Gluesenkamp et al. 2019 in which about 10% of the energy consumed by the dryer is consumed by sensible heating of drying components and the load itself. That sensible heating effect was thus neglected to enhance to clarity of this work.

### 2.4 Drum

For all ideal dryers considered in this work, the drum is assumed to be an adiabatic device in which the process air reaches saturation. Thermal masses are neglected. Together, these assumptions mean that the process air undergoes an isenthalpic process reaching its wet bulb temperature. This is similar to a model of a simple ideal evaporative cooling tower model.

### 2.5 Load and drying time

In order to present drying time intuitively in units of time, it is necessary to assume a cloth load size, starting moisture content, and ending moisture content. In this way, the non-dimensional dry time of Eqn. 2 can be dimensionalized to represent the drying time expected of a standard residential load at a typical tumble dryer air flow rate. The drying time can be expressed as in Eqn. 3 when we assume the following standard parameters: load dry weight  $m_c = 3.83$  kg (8.45 lb), load starting water mass ratio  $y_i = 57.5\%$ , load final water mass ratio  $y_f = 4\%$ , and mass flow rate of dry air  $\dot{m}_{dot,da} = 0.0646$  kg<sub>da</sub>/s. A dry air mass flow rate of 0.0646 kg<sub>da</sub>/s corresponds to 56.6 L/s (120 ft<sup>3</sup>/minute) volumetric air flow leaving the cold heat exchanger under typical operating conditions, which is a typical value for conventional residential electric resistance dryers. Equation 3 shows that the dry time is inversely proportional to the change in humidity ratio across the drum, and proportional to a scalar constant that represents the load size, starting moisture content, ending moisture content, and air flow rate.

$$\text{drying time} = \frac{m_c(y_i - y_f)}{\dot{m}_{dry\ air}(\omega_3 - \omega_2)} = \frac{3.83\text{ kg}_c(0.575 - 0.040)\text{ kg}_w/\text{kg}_c}{0.0646\frac{\text{kg}_{da}}{\text{s}}\Delta\omega\frac{\text{kg}_w}{\text{kg}_{da}}} = \frac{31.72}{\Delta\omega} \quad (\text{s}) \quad (3)$$

### 2.6 Air movement and ducting

All ducts (and connections among components) operate without leakage of air mass nor heat. Blower power is neglected.

In cases with an ambient HX, cases (a) and (c) in **Figure 1**, power associated with the pressure loss of moving fluid through the HX is neglected.

### 3. EFFICIENCY LIMITS FOR IDEAL DRYERS

In this work, two ideal ERDs are considered. It is assumed that electric resistance produces one unit of thermal energy for each unit of work energy consumed.

Two ideal HPDs are considered (unvented and vented). The Carnot cycle is characterized by a reversible heat pump that moves heat from a cold temperature  $T_C$  to a hot temperature  $T_H$ .

The results were computed numerically, due to the involvement of psychrometric property calls, which complicate the presentation of a closed-form analytical solution. Property calls and simultaneous equation solving were conducted in Engineering Equation Solver (EES) program (Klein 2016).

#### 3.1 Closed (unvented) ERD

In an ideal unvented ERD, **Figure 1(a)**, air circulates in a closed loop without leakage of mass nor heat. Heat is added by an electric resistance element (represented in the model by a hot heat exchanger, “Hot HX”). The air then flows through the drum, isenthalpically cooling and gaining moisture to its wet bulb temperature, and then heat is removed from the air by a heat exchanger (Amb HX) that cools the air below its dewpoint, dehumidifying the process air.

The system model can be solved by assuming steady state process air state points and using a psychrometric property lookup function. Steady state operation for the process air requires that the heat added be equal to the heat removed. Since the process air follows an adiabatic (isenthalpic) process in the drum, the only heat added to the system is  $Q$ , and the only heat removed is  $Q_{amb}$ ; thus  $Q = Q_{amb}$ . Additional constraints are imposed by the drum process (an adiabatic dehumidification to saturation, i.e. the wet bulb temperature).

The system is characterized by two degrees of freedom (Table 1). Both are up to the system designer: the amount of heat added to the air flow upstream of the drum, and the amount of heat removed from the air flow downstream of the drum. In the model in this work, T[2] and T[4] were chosen as the free variables, while noting the constraint that T[5] must stay above T[1].

#### 3.2 Open (vented) ERD

In an ideal vented ERD, **Figure 1(b)**, air is drawn from the surroundings, ducted to the heater and clothes, and then vented to ambient.

This system is the simplest of the four to solve, since there are only two processes to model and it is an open loop (no simultaneous equation solver is needed). It can be solved by using a psychrometric property lookup function for dry heat addition in the hot HX and the adiabatic dehumidification process to saturation in the drum.

The system is characterized by three degrees of freedom (Table 1). Two are environmental, corresponding to the ambient dry bulb and ambient humidity. One is up to the system designer: the amount of heat added to the air flow.

#### 3.3 Closed (unvented) HPD

In an ideal unvented HPD, **Figure 1(c)**, air circulates in a closed loop without leakage of mass nor heat. The air leaving the drum is cooled across a cold HX (at cold heat pump temperature  $T_C$ ) below the process air dewpoint, dehumidifying the process air. The condensate leaves the system. The dehumidified process air proceeds to the hot HX (at  $T_H$ ) where it is heated before re-entering the drum. According to an energy balance on the heat pump ( $W = Q_H - Q_C$ ), the hot HX capacity ( $Q_H$ ) is greater than the cold HX capacity ( $Q_C$ ). To prevent thermal runaway and achieve steady state operation, an exchange of heat to ambient is needed. While the exchange of heat to ambient could theoretically occur between any two state points, it was placed after the cold HX and before the hot HX to maximize performance, in keeping with the objective of modeling an ideal system.

The system can be solved by assuming steady state process air state points and using a psychrometric property lookup function. An energy balance on the process air requires that the heat added ( $Q_H$ ) be equal to the heat removed ( $Q_C + Q_{amb}$ ). Additional constraints are imposed by the drum process (an adiabatic dehumidification to saturation, i.e. the wet bulb temperature), and by an energy balance on the heat pump:  $Q_C + W = Q_H$ . In addition, the COP of the heat pump is defined as the Carnot heating COP:  $COP_{Cl,h} = T_H/(T_H - T_C)$ , where  $T_H = T[2]$  and  $T_C = T[4]$ . This set of constraints is enough to solve the system, when the two degrees of freedom are assigned values.

The system is characterized by two degrees of freedom (Table 1). Both are controllable by the system designer, with the constraint that  $T[5]$  stay above  $T[1]$ . The two degrees of freedom can be characterized as the amount of heat added to the air flow upstream of the drum, and the amount of heat removed from the air flow downstream of the drum. In the model in this work,  $T[2]$  and  $T[5]$  were chosen as the free variables. In this work,  $T[5]$  was chosen as a free variable instead of  $T[4]$ . This choice was made because using  $T[5]$  as the free variable enhances solver stability, since the constraint imposed by  $T[1]$  acts directly on  $T[5]$ , and only indirectly on  $T[4]$ .

### 3.4 Open (vented) HPD

In an ideal vented HPD, **Figure 1(d)**, air is drawn from the surroundings, ducted to the hot HX (at  $T_H$ ), proceeds to the drum, transfers heat to the cold HX (at  $T_C$ ), and is then vented to ambient.

The system can be solved by assuming steady state process air state points and using a psychrometric property lookup function. Additional constraints are supplied by the drum process (an adiabatic dehumidification to saturation, i.e. the wet bulb temperature), and an energy balance on the heat pump:  $Q_C + W = Q_H$ . In addition, the COP of the heat pump is a constraint:  $COP_{Cl,h} = T_H/(T_H - T_C)$ , where  $T_H = T[2]$  and  $T_C = T[4]$ . This set of constraints is enough to solve the system, when the remaining degrees of freedom are assigned values.

The system is characterized by three degrees of freedom (Table 1). Two are environmental, corresponding to the ambient dry bulb and ambient humidity. One is up to the system designer: the amount of heat added to the air flow.

The degrees of freedom for each system type are summarized in Table 1.

**Table 1:** Analysis of the degrees of freedom for each system type

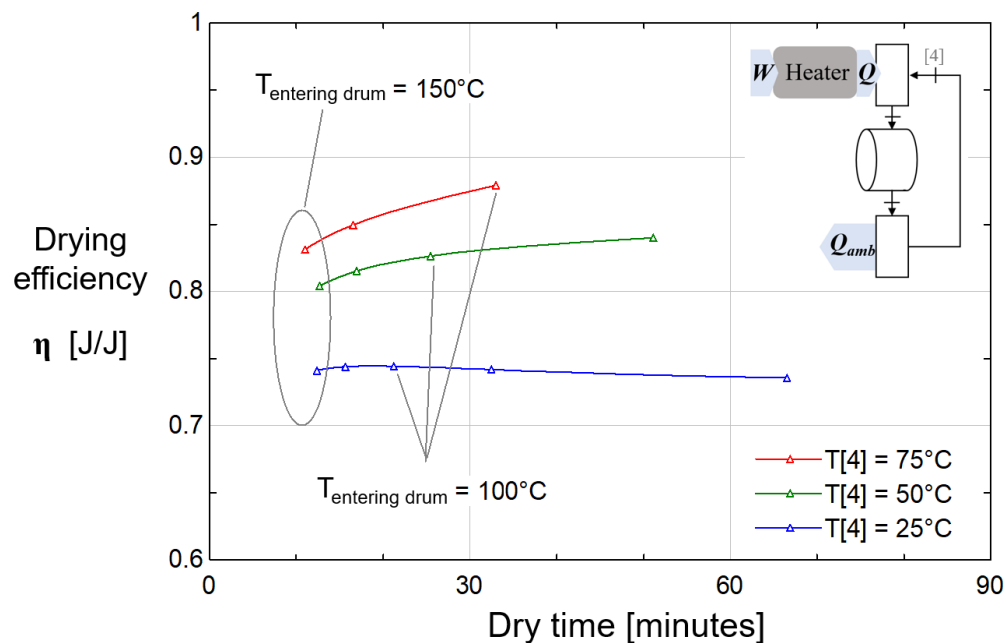
System type	Total count of degrees of freedom	Uncontrollable (environment-related) degrees of freedom		Controllable (design-related) degrees of freedom		Notes
		Count	List	Count	List of free variables chosen in this work	
Closed (unvented) electric resistance dryer	2	0	–	2	$T[2]$ drum inlet $T[4]$ coldest point	The ambient temperature $T[1]$ imposes a lower limit on $T[4]$
Open (vented) electric resistance dryer	3	2	$T[1]$ $RH[1]$	1	$T[2]$ drum inlet	
Closed (unvented) Carnot heat pump dryer	2	0	–	2	$T[2]$ drum inlet $T[5]$ coldest point	The ambient temperature $T[1]$ imposes a lower limit on $T[5]$
Open (vented) Carnot heat pump dryer	3	2	$T[1]$ $RH[1]$	1	$T[2]$ drum inlet	

## 4. RESULTS

This section shows computed performance of the four dryer types. There are two metrics of interest (efficiency and dry time), and either 2 or 3 independent variables (2 for the unvented systems, and 3 for the vented systems). All results are plotted as the efficiency versus the dry time. For the unvented systems with 2 independent variables, visualizing the results is straightforward, and a range of drum entering temperatures from 25 to 150°C is shown for three cycle minimum temperatures. For the vented systems with 3 independent variables, multiple plots were used to keep each plot uncluttered. Drum entering temperatures ranging from 25 to 150°C are again shown, for three ambient dry bulb temperatures. The effect of ambient humidity is shown with separate plots for each humidity level.

### 3.1 Closed (unvented) ERD

The unvented ERD efficiency and dry time are functions of two free variables: the drum inlet temperature and how far the process air is cooled before it re-enters the heater. Figure 2 parameterizes these two variables to portray the efficiency and dry time of the Carnot system.



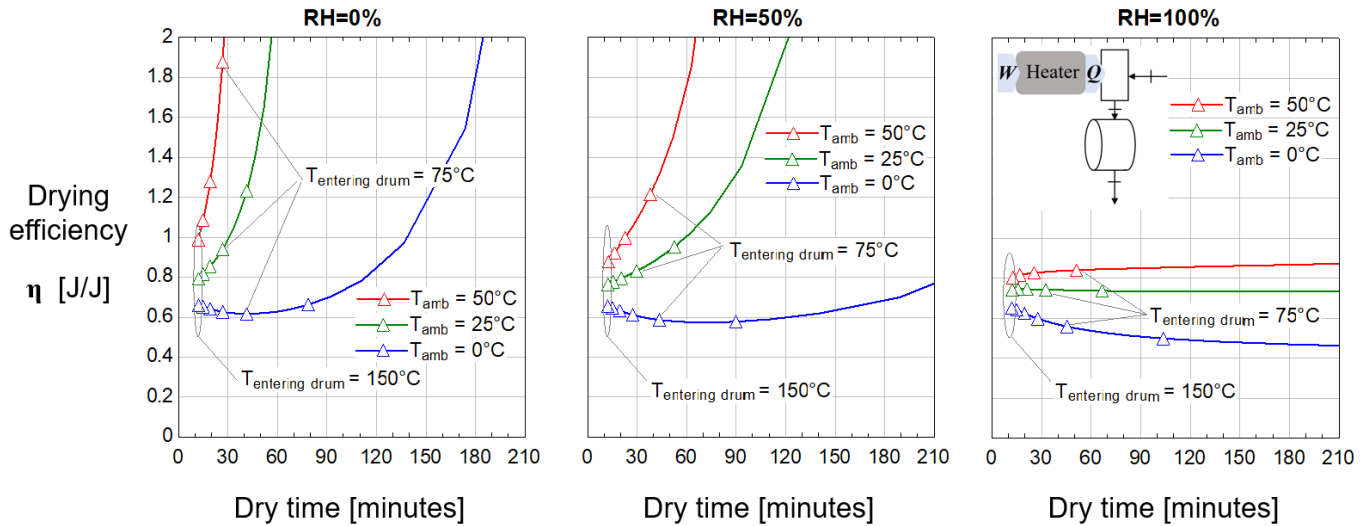
**Figure 2:** The efficiency and dry time of an ideal unvented ERD (Fig 1a). Drum entering temperatures are shown in 25°C increments.

Figure 2 shows that dry time depends strongly on entering drum temperature. Efficiency is relatively insensitive to entering drum temperature. Slightly higher efficiency can be achieved by elevating the entire cycle temperature, but that lengthens dry time, and the efficiency advantage may disappear when thermal mass is accounted for.

### 3.2 Open (vented) ERD

The vented ERD performance is a function of three free variables. These are varied parametrically in Figure 3.





**Figure 3:** The efficiency and dry time of an ideal vented ERD (Fig 1b). Drum entering temperatures are shown in 25°C increments.

By analysis of Figure 3, it's clear that lower ambient humidity results in both faster dry time and higher efficiency. In addition, efficiency greater than 1 is possible. For a standard ambient condition,  $T_{amb} = 25^{\circ}\text{C}$  and  $RH_{amb} = 50\%$ , dry times longer than an hour can achieve efficiency greater than 100%, and heatless drying can be achieved in 3 hours with infinite efficiency.

### 3.3 Closed (unvented) HPD

The unvented HPD efficiency and dry time are functions of two free variables: the drum inlet temperature and how far the process air is cooled before it re-enters the heater. Figure 4 parameterizes these two variables to portray the efficiency and dry time of the Carnot system.

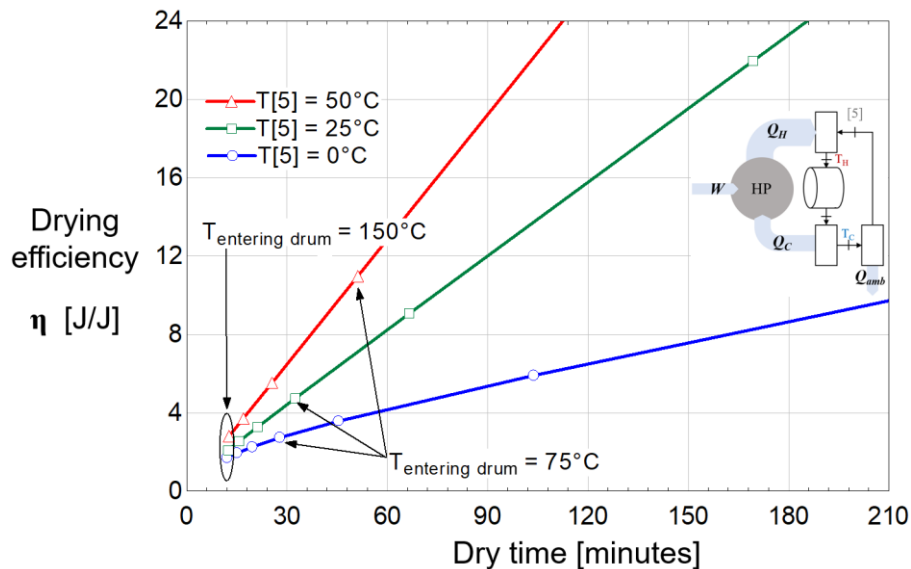


**Figure 4:** The efficiency and dry time of an unvented Carnot HPD (Fig 1c). Drum entering temperatures are shown in 25°C increments.

Figure 4 shows that elevating the cycle temperature can improve efficiency, but at the expense of longer dry time.

### 3.4 Open (vented) HPD

The vented HPD performance is a function of three free variables. These are varied parametrically in Figure 5.

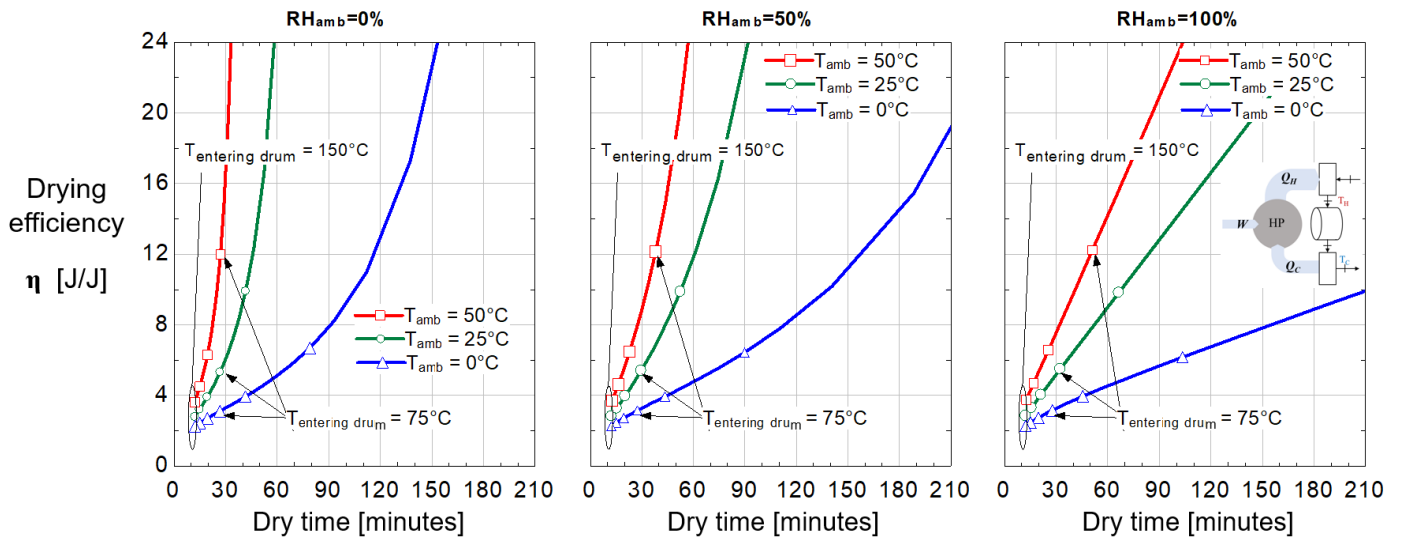


**Figure 5:** The efficiency and dry time of a Carnot vented HPD (Fig 1d). Drum entering temperatures are shown in  $25^\circ\text{C}$  increments.

Comparing Figure 5 to Figure 4 shows that efficiency and dry time are generally more favorable for the vented system, and that the vented system performs similarly to unvented as the ambient humidity approaches 100%.

## 5. DISCUSSION AND CONCLUSIONS

Open (vented) systems have only one free variable available to the system designer, but depend on two uncontrolled variables (ambient dry bulb temperature and ambient humidity). The design choice left to the cycle designer is the size of the heat pump (that is, how much heat to add,  $Q_H$ ). The drum entering temperature is directly determined by the heat pump size relative to air flow rate: for every 10 K of temperature rise desired, the  $Q_H$  should be 10 W per gram per second of air flow (or about 578 W per 100 CFM for every 10 K temperature rise).

Closed (unvented) systems have two free variables available to the designer, and are only weakly coupled to ambient dry bulb. For the ideal unvented cases, ambient RH does not influence the system. The system designer can control the drum entering temperature separately from the heater size. For example, a high drum temperature can be achieved with a small heat pump by restricting the quantity of heat rejected to ambient. Raising the process air temperature in this way can lead to faster dry times with higher efficiency.

Thermal mass was neglected in this work, and in that context the efficiency and dry time of an unvented system can be improved by elevating the temperature of the entire air cycle. When thermal mass is considered, the benefits of elevated temperature operation will be lessened.

Despite unvented systems having the advantage of greater design control, their performance limits are lower (lower efficiency and longer dry time) than vented systems. This is because unvented systems don't take advantage of the evaporation potential of unsaturated ambient air. As ambient air approaches saturation (100% RH), unvented performance converges with vented performance.

## NOMENCLATURE

ERD	electric resistance dryer
$h_{fg}$	latent heat of vaporization of water
HPD	heat pump dryer
HX	heat exchanger

$m$	mass	
$\dot{m}$	mass flow rate	
RH	relative humidity	
$T$	temperature	(°C) or (K)
$Q$	heat transfer	(kW)
$W$	work	(kW)
$\omega$	humidity ratio	(g <sub>water</sub> /g <sub>dry air</sub> )

**Subscript**

$1$	state point 1: ambient	$c$	cloth
$2$	state point 2: entering drum	$C$	cold
$3$	state point 3: exiting drum	$da$	dry air
$4$	state point 4: see Fig. 1	$evap$	evaporation
$5$	state point 5: see Fig. 1	$H$	hot
$amb$	ambient	$w$	water

**REFERENCES**

- Cao, Xiang, Jing Zhang, Zhen-Yu Li, Liang-Liang Shao, Chun-Lu Zhang (2021). "Process simulation and analysis of a closed-loop heat pump clothes dryer," *Applied Thermal Engineering*, v. 199, 117545, DOI: <https://doi.org/10.1016/j.applthermaleng.2021.117545>
- Gluesenkamp, Kyle R.; Philip Boudreaux, Viral Patel, Dakota Goodman, Bo Shen (2019). "An efficient correlation for heat and mass transfer effectiveness in tumble-type clothes dryer drums," *Energy*, v. 172, 1225-1242 (April 2019). <https://doi.org/10.1016/j.energy.2019.01.146>
- Gluesenkamp, Kyle R., Viral K. Patel, Ayyoub M. Momen (2020). "Efficiency Limits of Evaporative Fabric Drying Methods," *Drying Technology*, (November) DOI: <https://doi.org/10.1080/07373937.2020.1839486>
- Klein, S.A., Engineering Equation Solver, 2016, F-Chart Software.
- Lee, Bing-Hung, Rony A. Sian & Chi-Chuan Wang (2019). "A rationally based model applicable for heat pump tumble dryer," *Drying Technology*, 37:6, 691-706, DOI: 10.1080/07373937.2018.1454940
- Lee, Dongchan, Minwoo Lee, Myeong Hyeon Park, Yongchan Kim (2022). "Experimental evaluation and prediction model development on the heat and mass transfer characteristics of tumble drum in clothes dryers," *Applied Thermal Engineering*, v. 202, 117900, DOI: <https://doi.org/10.1016/j.applthermaleng.2021.117900>.
- Peng, Z-R, Wang, G-B, Zhang, X-R. (2019). "Thermodynamic analysis of novel heat pump cycles for drying process with large temperature lift," *Int J Energy Res*, v. 43, pp. 3201– 3222, DOI: <https://doi.org/10.1002/er.4394>
- Sian, Rony A., Chi-Chuan Wang (2019). "Comparative study for CO<sub>2</sub> and R-134a heat pump tumble dryer – A rational approach," *International Journal of Refrigeration*, v. 106, pp. 474-491, DOI: <https://doi.org/10.1016/j.ijrefrig.2019.05.027>

**ACKNOWLEDGEMENT**

This work was sponsored by the U. S. Department of Energy's Building Technologies Office under Contract No. DE-AC05-00OR22725 with UT-Battelle, LLC. This research used resources at the Building Technologies Research and Integration Center, a DOE Office of Science User Facility operated by the Oak Ridge National Laboratory. The authors would like to acknowledge Wyatt Merrill, Technology Manager, U.S. Department of Energy Building Technologies Office. The authors also acknowledge helpful review comments from Philip Boudreaux.